1) 四肢や体幹での筋力・関節可動域の維持改善

2) 四肢の関節や脊柱における変形の予防と軽減化

3) 日常生活動作における能力の維持改善（自助具，下肢装具，座位保持装置，車椅子などを処方，作製）

4) 社会生活における環境の調整（自宅，学校，職場での生活環境の改善，すなわち玄関，部屋，トイレ，風呂場，ベッド，机，食堂などの改良）

5) 家族などの介護労作の軽減

6) 精神的援助による生活意欲の向上や余暇活動の援助による生活の質の充実

2. 筋ジストロフィーの理学療法

筋ジストロフィーでは，進行すると四肢や体幹の拘縮は必ず起こる．予防によって変形や拘縮は努力によってある程度阻止することは可能である．その予防には早期からの関節可動域訓練や，筋のストレッチを行う．そして、筋力の低下した筋を積極的に動かし維持・増強をはかることも動作能力の維持にとって重要である．以下、理学療法での目的を列挙する。

1) 歩行を中心とした起居移動動作能力を可能な限り維持または改善する．

2) 四肢，体幹の変形や拘縮の発生を予防・増悪阻止する．

3) 筋力を可能な限り長期にわたって維持または増強する．

4) 装具，車椅子，電動車椅子の適応により移動能力を維持・再獲得する．

5) 呼吸機能障害の進行を可能な限り遅延させる．

C．研究結果

以上述べた筋ジストロフィーのリハビリテーションプログラムおよび理学療法からロボットスーツの適用可能性について検討する。

1. ロボットスーツによる各種動作訓練

1.1. 起居移動動作補助・訓練および起立歩行補助・訓練

障害の進行とともに歩行不能となり車椅子を使用するようになると，急速に四肢や体幹の変形が発生・増悪してきやすくなるので，可能な限り起立歩行期間を維持しなければならない．これに関しては、患者の障害のレベルに合わせロボットスーツのアシスト出力を調整することによって患者の起居移動動作および起立歩行の支援を実施する。これにより障害の進行を遅らせることが見込まれる。

1. 2. ストレッチ（伸張訓練），関節可動域訓練

関節の運動範囲の増大・維持を目的とする訓練であり、変形や拘縮の発生を遅らせると起居移動動作能力をより長く維持することが可能となる。ロボットスーツには力センサおよび角度センサが付いているので、関節にどのくらいの力をかければよいのかを把握することが出来る。これにより介助者なしで、定量的なストレッチ、可動域訓練が可能となる。

1.3. 筋力維持訓練

進行による筋力低下だけでなく活動量が少なくなることで筋肉の不使用による筋力低下や萎縮がさらに増悪します．この不使用に対する筋力低下を予防する筋力訓練はある程度効果ある．ロボットスーツは支援することだけではなく、装着者に負荷をかけるトレーニング的な仕様（抵抗運動）も可能であり、また、ロボットスーツは筋力を定量的にモニタリングすることが可能であるため、筋ジストロフィー患者の筋力レベルに応じた訓練を効果的に実施することができる。

2. 実証実験

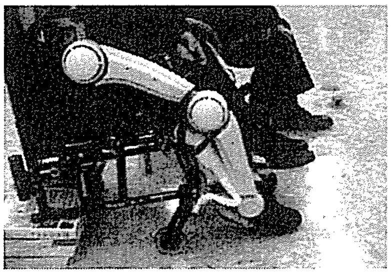

(a)

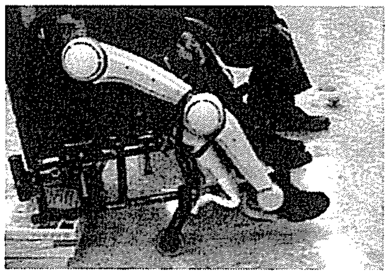

(b)

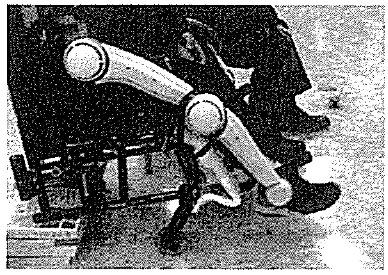

(c)

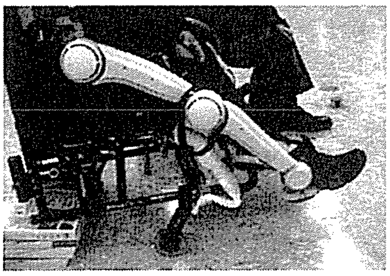

(d)

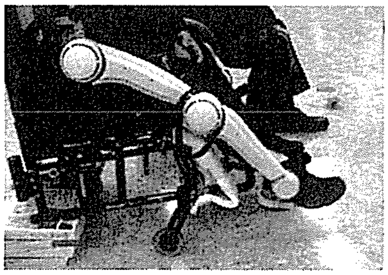

(e)

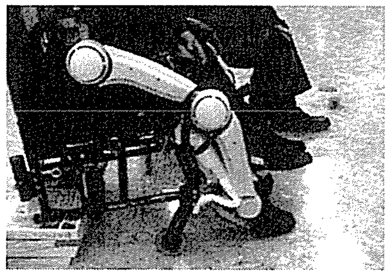

(f)

図１　膝関節の屈曲伸展動作訓練

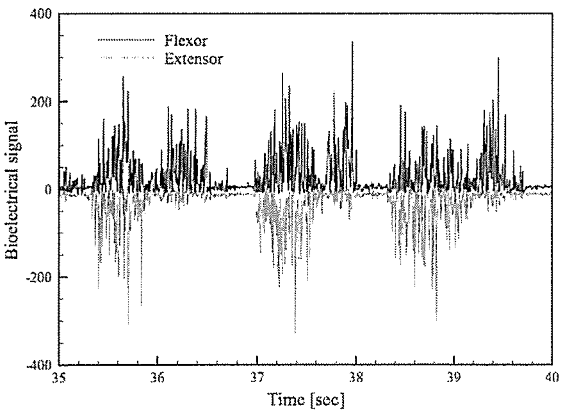

(a)　生体信号

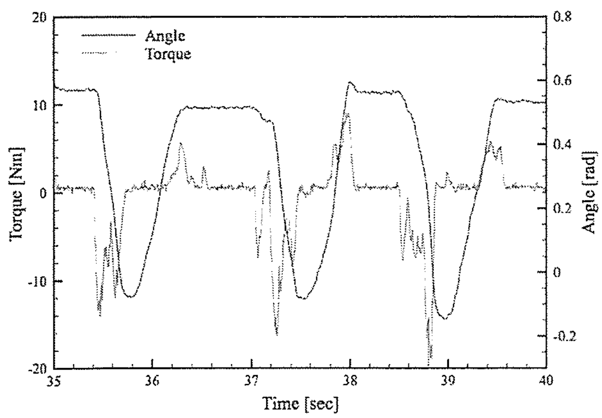

(b)　アシストトルク・角度

図２　実証実験結果

キンジストロフィーを有する方に協力していただき、膝関節屈曲伸展動作を試みた。実験の様子を図１(a)ー(f)、図２に実験データを示す。

D．考察

ロボットスーツは装着者の力を補助するという従来型のパワーアシスト装置とは異なり、「筋発生力等の身体機能の診断」、「適応リハビリテーション」、「随意・自律のハイブリット制御による動作支援」を一台で行うことができる装置であり、「起居移動動作補助・訓練および起立歩行補助・訓練」、「ストレッチ（伸張訓練），関節可動域訓練」、「筋力維持訓練」等筋ジストロフィーの進行を遅らせるために重要な支援・訓練を効果的に実施することができることが分かった。また、簡単な実証実験では、装着者の生体信号に応じて、ロボットスーツが制御されていることを確認した。今後は、筋ジストロフィー患者の進行状況に合わせ

たリハビリテーション・運動支援手法を提案し、患者のＱＯＬを向上させる手法検討する。

E．結論

本研究では筋ジストロフィー患者のリハビリテーションの現状からロボットスーツの適用可能性について検討した。ロボットスーツの機能を利用することにより、筋ジストロフィーの進行を遅らせるために必要な運動訓練・支援に適用の可能性があることが分かった。また、簡単な実証実験を試み、装着者の運動意思に応じてロボットスーツを使って膝関節屈曲伸展動作を実施することができた。

F．研究発表

1．論文発表

[1] 中島孝, 難病のQOL向上–QOL評価と緩和ケア，日本難病看護学会誌，11巻1号，pp. 33-34, 2006

[2] 阿部康二編集, 中島孝, 神経難病のQOL評価から緩和ケアについて, 神経内科のすべて, 新興医学社, 2006

[3] 伊藤博明, 中島孝, 神経内科の医療・介護—現状と課題, 在宅神経難病患者のQOL, 神経内科, 12月号, 2006

[4] 坂井健二, 中島孝, 福原信義, 抗凝固治療開始後にmicoroembolic signalの一過性増加をみとめた原発性抗リン脂質抗体症候群の一例, 脳と神経, 58(5), 439-42, 2006

[5] 中島孝, QOL向上とは, 難病のQOL評価と緩和ケア, 脳と神経, 58(8):661-669, 2006

G. 知的財産権の出願・登録状況

1．特許取得

なし。

2．実用新案登録

なし。

3．その他

なし。

III. 研究成果の刊行に関する一覧表

書籍

著者氏名	論文タイトル名	書籍全体の編集者名	書籍名	出版社名	出版地	出版年	ページ
居村茂幸	第12章リスク管理	吉尾雅春	標準理学療法学＜専門分野＞運動療法学各論 第2版	医学書院		2006	400-407
居村茂幸		内山靖	理学療法学事典	医学書院		2006	
居村茂幸		居村茂幸	系統理学療法学 筋骨格障害系理学療法学	医歯薬出版		2006	
居村茂幸	内部障害と理学療法アプローチ	居村茂幸	系統理学療法学 内部障害系理学療法学	医歯薬出版		2006	1-4
居村茂幸	呼吸機能の障害と理学療法	居村茂幸	系統理学療法学 内部障害系理学療法学	医歯薬出版		2006	5-21
中島孝	神経難病のQOL評価から緩和ケアについて	阿部康二	神経内科のすべて	新興医学社	東京	2006	
	ロボットスーツHAL		ニュートンムック 明日を一新する「値千金」の技術32	ニュートンプレス出版	東京	2006	150-151
	コラムNo. 03 装着型ロボット（筑波大学開発のロボットスーツHAL）		平成18年版科学技術白書	文部科学省	東京	2006	26
	腕力・筋力が数倍アップする？　夢のロボットスーツ実用化へ		ダカーポ587号	マガジンハウス	東京	2006	41
	「人のパワーをアップしてくれる！」		チャレンジ４年生わくわく発見ブック	ベネッセコーポレーション	東京	2006	7
	″解体″され始めたロボット		知恵蔵2007	朝日新聞社	東京	2006	686
	ロボットスーツ開発にわくわく		朝日中学生ウィークリー	朝日新聞社	東京	2006	1

雑誌

発表者氏名	論文タイトル名	発表誌名	巻名	ページ	出版年
H.Toda, T. Kobayakawa, Y. Sankai	A multi-link system control strategy based on biological reaching movement	Advanced Robotics	20(6)	661-679	2006
河本浩明, 塚原淳, 山海嘉之	人間の動作特性を考慮したロボットスーツＨＡＬによる立ち上がり動作支援に関する研究	第7回計測自動制御学会システムインテグレーション部門学術講演会(SI2006)		345-346	2006
Kenta Suzuki, Gouji Mito, Hiroaki Kawamoto, Yasuhisa Hasegawa, Yoshiyuki Sankai	Intention-Based Walking Support for Paraplegia Patients with Robot Suit HAL	Advanced Robotics	21(13)	印刷中	2007
間瀬教史, 居村茂幸, 北川薫	下肢の骨関節疾患患者の筋力回復と筋線維伝導速度との関係	理学療法学	33 (Suppl.2)	293	2006
Kyoshi Masae, Hiromitsu Kamimura, Shegeyuki Imura, Kaoru Kitagawa	Effect of Age and Gender on Muscle Function –Analysis by Muscle Fiber Conduction Velocity	J. Phys. Ther. Sci.	18	81-87	2006
中島孝	QOL評価の新しい挑戦ｰ療養者の物語によるSEIQoL-DWの試みｰ	日本難病看護学会誌	11巻 1号	33-34	2006
伊藤博明、中島孝	在宅神経難病患者のQOL	神経内科	12月号		2006
中島孝	難病のQOL評価と緩和ケア	脳と神経	58(8)	661-669	2006
Nakajima T.	Individual ALS care in the Japanese ‘nanbyo’care model: comparison with palliative care approaches in achieving best quality of life	Amyotrophic Lateral Sclerosis	Suppl 1 7	45–47	2006
土井将弘, 松野隆幸, 長谷川泰久, 福田敏男	点接触の仮定に基づく2足歩行のLateral運動制御	日本機械学会論文集（C編）	７２巻７１８号	1832-1839	2006
Hideki Kajima, Yasuhisa Hasegawa, Masahiro Doi, Toshio Fukuda	Energy-based Swing-back Control for Continuous Brachiation of Multi-Locomotion Robot	International Journal of Intelligent Systems	Vol.21, No.9	1025-1043	2006

平成１８年度　研究成果の刊行に関する一覧表

雑誌

板原達也，葛岡英明，山下淳，山崎敬一，中村裕一，尾関基行	対話型作業支援システムにおけるロボットの補助効果に関する研究	情報処理学会論文誌	Vol.48, No.2	印刷中	2007
秋谷直矩，丹羽仁史，坪田寿夫，鶴田幸恵，葛岡英明，久野義徳，山崎敬一	介護ロボット開発に向けた高齢者介護施設における相互行為の社会学的分析	電子情報通信学会誌	Vol.J90-D No.3	798-807	2007
	人間の出せない能力をサポートする「モビルスーツ」か	最新科学おもしろ雑学帖	4月号	182	2006
	夢背負うロボットスーツ	読売新聞	4月3日	34	2006
	ロボット着ておんぶ登山	朝日新聞	4月3日	30	2006
	「ロボットスーツ」歩行支援用商品化	朝日新聞	4月11日		2006
	ロボットスーツ　抱っこもひょいっと	朝日新聞	5月24日	38	2006
	ロボットで身体機能拡張	日経産業新聞	6月7日	9	2006
	ロボスーツきょう出発,	信濃毎日新聞	7月31日	26	2006
	Hal-5　l’armure bioniquep	SCIENCE&VIE decouvertes	2006年8月号	18	2006
	ロボットスーツ登山 夢のアルプス挑戦控え「幸せ」	信濃毎日新聞	8月5日	6	2006
	ロボスーツでおんぶ　アルプス４千メートル峰へ,	朝日新聞	8月8日	30	2006
	「グッドデザイン」大賞は？	朝日新聞夕刊	10月13日	6	2006
	ロボットスーツ実用化 筑波大学発、介護などに期待	読売新聞	10月29日		2006
	Esqueleto bionico:HAL-5,	Peru21	12月26日		2006
	Shaping our future along with robots	The Japan Times	12月31日	14	2006
	Rise of the body bots	ENGINEERING WORLD		1, 8-13	2007
	ロボットが生活の身近に小型・省エネ・高機能化進む	日本経済新聞	1月1日	元旦第六部, pp. 3	2007
	ロボットスーツ：おかえりHAL-5,	毎日新聞	1月12日	8	2007
	デジタル最前線突撃レポート　ロボットスーツ「HAL」	Saai Isara	2月号	26-29	2007

平成１８年度　研究成果の刊行に関する一覧表

雑誌

	世界が注目する日本のロボティクス最前線　ロボットスーツHAL-5	ロボットライフ	3月号	24-31	2007
	ロボット大国日本の新潮流　世界初の歩行を助けるロボットスーツ	nature DIGEST日本語編集版	2月号	18-20	2007
	広がりをみせるデザインの方向性　温かみのある医療機器デザイン	TIME&SPACE	2・3月号	6	2007
	着るロボ家庭に	日本経済新聞	2月15日	3	2007

IV. 研究成果の刊行物・別刷り

Advanced Robotics, Vol. 20, No. 6, pp. 661–679 (2006)

Also available online - www.vsppub.com

Full paper

A multi-link system control strategy based on biological reaching movement

HIDEKI TODA [1], TATSU KOBAYAKAWA [2] and YOSHIYUKI SANKAI [1,*]

[1] *Doctoral Program of Systems and Information Engineering, Sankai Laboratory, University of Tsukuba, Tsukuba, Ibaraki 305-0006, Japan*
[2] *Multimodal Integration Research Group, Institute for Human Science and Biomedical Engineering, National Institute of Advanced Industrial Science and Technology, AIST Tsukuba Central 6, Tsukuba, Ibaraki 305-8561, Japan*

Received 12 May 2005; accepted 22 July 2005

Abstract—In the multi-link arm control process, the problems of trajectory planning and trajectory realization have been recognized as being of key importance. We developed a technique by which to realize a reaching movement control of the multi-link arm system, which was inspired by experimental results for reaching movements of macaques or human beings. The proposed method can treat the effect of the dynamics of the multi-link system and the trajectory planning of the end-effector, which has a bell-shaped speed profile, as well as the difficulties of redundancies of multi-link systems. Two-link arm reaching movement experiments revealed the same features, as demonstrated by the results of biological experiments on humans and macaques. In addition, the results obtained using a two-dimensional four-link model in a standing-up movement control experiment agreed well with 'standing-up from a chair' movement of human beings. Since the proposed method has a simple structure and its implementation process is simple, the proposed method will be effective for use in a multi-link system control strategy.

Keywords: Multi-link control; biologically inspired control; bell-shaped speed profile.

1. INTRODUCTION

Many creatures, including human beings, realize movement through multi-link systems, or what are usually referred to as 'arms' or 'legs'. Interpreting the control planning and executive system of a creature as a control system is useful for understanding the control strategy of the cerebellum as well as for application to machine systems used by humans, e.g., walking assist systems [1] or artificial limbs (Fig. 1).

*To whom correspondence should be addressed. E-mail: sankai@golem.kz.tsukuba.ac.jp

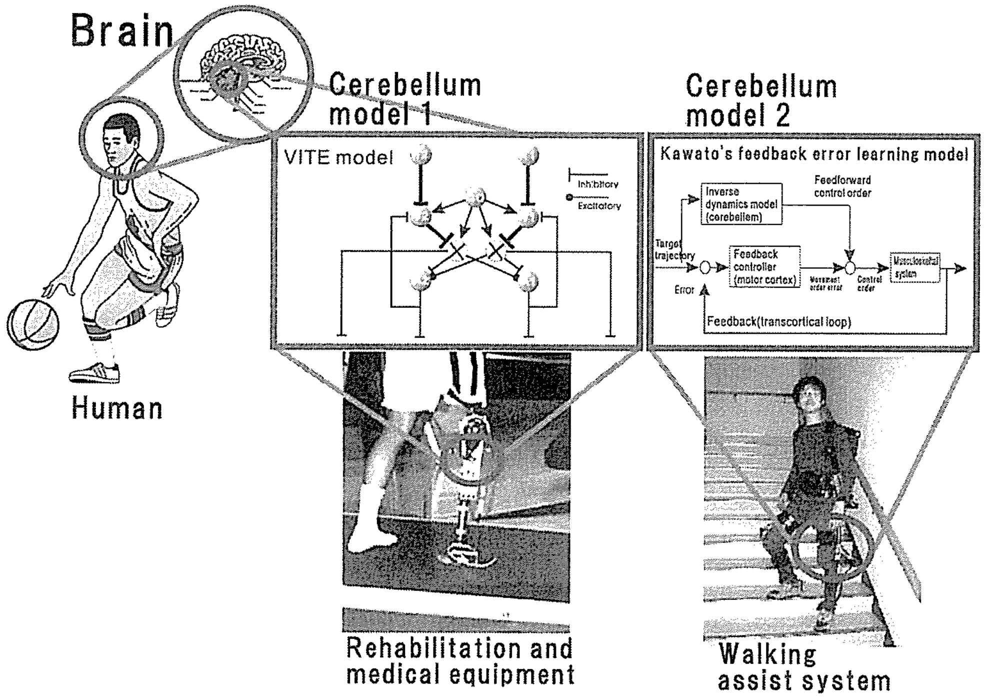

Figure 1. Mathematical approach based on biological models.

Manipulator control has been investigated for decades [2]. Volpe and Khosa [3] show that general impedances are useful for manipulator control, and a neural oscillator model [4] has been used to exploit the intrinsic dynamics of the control process. Approaches involving the cerebellum model [5–7] have been used for motion creation and as a control model. Studies of the kinematic and dynamic aspects of the planar, unconstrained multi-link arm movements of humans and monkeys [8, 9] have shown some features such as:

- Straight-line hand trajectory.
- Single-peaked, bell-shaped speed profile of hand trajectory.

Bernstein [10] stated that there are three problems in multi-link system movement control. The first involves how the central nervous system (CNS) selects a specific hand trajectory from the infinite number possibilities in moving from one point to another. The second involves how the CNS determines the joint angle combinations in order to realize the hand trajectory. The third involves how the CNS realizes the desired trajectory by giving motor control commands to the muscles. Trajectory planning and the trajectory realization process are ill-posed problems and a unique solution to these problems cannot be found.

From a biological perspective, a number of biomechanics models for multi-link system control have been proposed, including the VITE/FLETE model by Bullock and Grossberg [11], the equilibrium point hypothesis/control theory [12–14] and the minimum torque change criterion model, proposed by Kawato *et al.* [15] and Uno *et al.* [16]. Biological experiments examining monkey elbow movements have indicated that the CNS generates control signals that define a series of equilibrium positions [17] and Feldman [18] realized two-link arm reaching movement control by using the equilibrium point hypothesis/control theory. According to the equilibrium point hypothesis, Hogan [19] used the 'minimum jerk criterion' rule to determine an ideal trajectory plan from the initial position to the final position of the arm which had a 'bell-shaped' speed profile property. Generally, movement control is constructed from two execution processes, which are divided into each other functionally. The first process is trajectory planning, which corresponds to the VITE model and the minimum jerk criterion rule. The second process is the movement realization process, the FLETE model and a kind of torque criterion or torque smoothness cost function that is used in conjunction with the model. The trajectory planning process is treated using static trajectory planning algorithms, which depend on work space coordinates and are independent of the dynamics of the multi-link system. In addition, these two problems are not clearly separable. Therefore, rather than handling the two processes using different algorithms, we propose a controller that has a trajectory generating function. In this controller, the force decision process is executed while performing the trajectory planning process.

2. THEORY

A diagram of the proposed multi-link system controller is shown in Fig. 2. The system controller is constructed from a trajectory planning controller and a trajectory realization controller. These two controllers receive the position, velocity and acceleration information of the end-effector of a multi-link system. The trajectory planning controller uses this information to decide the ideal trajectory of the end-effector as the force $\vec{f}$ of the end-effector and the trajectory realization controller uses this information to determine all of the joint torques $\vec{\tau}$ of the multi-link system. The proposed controller realizes multi-link reaching movement using

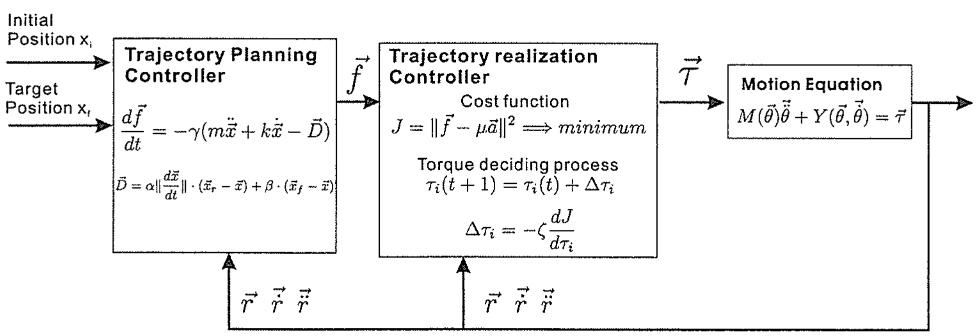

Figure 2. Block diagram of the proposed trajectory planning and realization.

only the acceleration of the end-effector. This mechanism can reduce the controller design complexity compared to previously proposed techniques, such as that of Ma [20]. However, instabilities due to simplicity must be avoided. The proposed controller manages instability by using a controller having the function of trajectory generation. In addition, the trajectory realization controller also determines the joint torques using only the acceleration of the end-effector and instabilities such as inverse kinematics are managed by the trajectory planning controller. In many cases, a previously proposed multi-link system controller is used to calculate the static ideal trajectory plan before the movement and multi-link movement is realized by following the calculated ideal trajectory plan (e.g., Fagg *et al.* [5]). This mechanism, however, has disadvantages for external disturbances and a calculation error of the inverse kinematics of the multi-link dynamics. The strategy of the proposed method does not realize the multi-link movement by resolving the inverse kinematics of the system and then controlling all of joints angles to previously calculated joint angles. Rather, the proposed method conveys only the end-effector position of the multi-link system from the initial position to the target position by using the acceleration information of the end-effector.

2.1. Trajectory planning controller

The proposed controller determines the present control order by using the information of the present hand position and the speed vector of the end-effector in the work space. We defined the control rule as follows:

$$\vec{f}^{\,\mathrm{bell}} = \alpha \left\| \frac{\mathrm{d}\vec{x}}{\mathrm{d}t} \right\| \cdot (\vec{x}_\mathrm{r} - \vec{x}) + \beta \cdot (\vec{x}_\mathrm{f} - \vec{x}), \tag{1}$$

where α and β are positive small constants, $\vec{f}$ is the force vector of the end-effector of the hand, and $\vec{x}$, $\vec{x}_\mathrm{i}$ and $\vec{x}_\mathrm{f}$ are the present initial and final positions of the end-effector of the hand, respectively. We herein set $\vec{x}_\mathrm{r} = (\vec{x}_\mathrm{i} + \vec{x}_\mathrm{f})/2$ as the reference position. Through an experiment examining reaching movement control in one-dimensional (1D) space, we confirm the validity of (1) by comparison with the PD control method.

The motion equation of a particle in 1D space is $m(\mathrm{d}^2x/\mathrm{d}t^2) = -k(\mathrm{d}x/\mathrm{d}t) + f_x$, where x, m and k are the position, mass and coefficient of friction of the system, respectively. In this case, we define $f_x = \alpha\|\mathrm{d}x/\mathrm{d}t\| \cdot (x_\mathrm{r} - x) + \beta \cdot (x_\mathrm{f} - x)$ from equation (1). The position, velocity and force of the proposed controller are shown in Fig. 3 for the case in which $m = 5$, initial position $x_\mathrm{i} = 0$, final position $x_\mathrm{f} = 10$, time step $\Delta t = 0.001$, $\alpha = 1.0$, $\beta = 0.001$ and $k = 0$.

The primary differences from the simple PD controller are the velocity and force profiles. The velocity distribution of the proposed controller has a symmetric bell-shape and the force has a reverse distribution at the reference point (x_r). These features are not seen in the simple PD controller.

For further clarification, we compared the proposed controller (Fig. 4) with the LQR controller (Fig. 5) under the condition of the 1D reaching movement

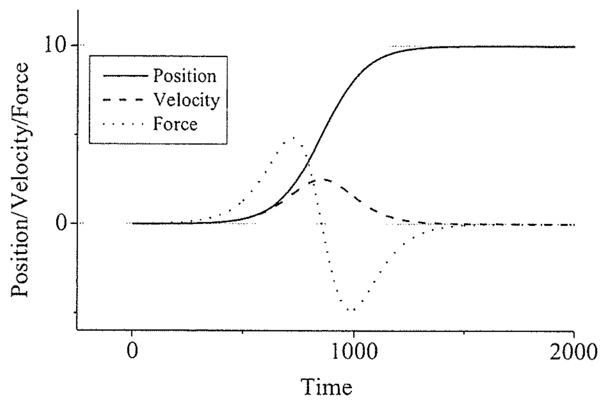

Figure 3. One-dimensional reaching movement of the proposed controller.

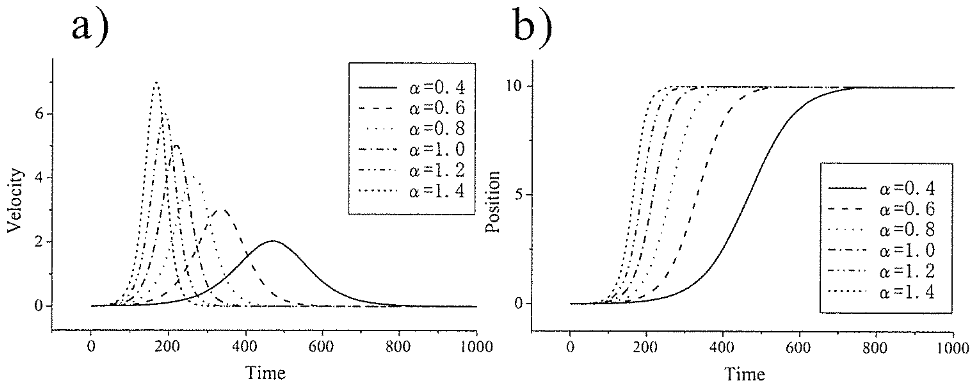

Figure 4. Parameter dependency of our proposed speed profile control method on (a) velocity and (b) position.

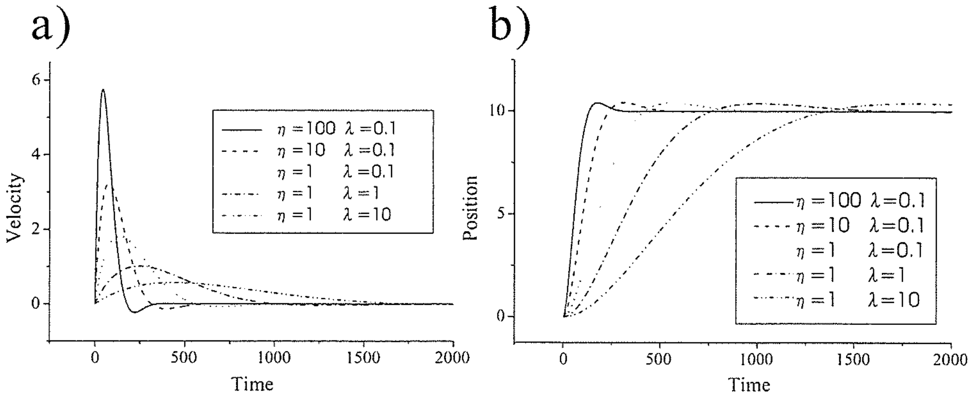

Figure 5. Parameter dependency of the LQR method on (a) velocity and (b) position transition.

($m = 20, k = 0, \Delta t = 0.001, x_i = 0, x_f = 10$). Here, we set a cost function as $J = \int_0^{t_f} \vec{x}^T Q \vec{x} + \vec{u}^T R \vec{u}\, dt$, where

$$Q = \begin{bmatrix} \eta & 0 \\ 0 & 1/\eta \end{bmatrix}$$

and $R = \lambda$. In this experiment, the LQR controller is defined as $f_x^{PD} = K_p(x_f - x) + K_d \dot{x}$, and we set the feedback gain K_p and K_d for minimizing the cost function Q in the case of constant parameter η, λ:

$$\begin{bmatrix} \eta \\ \lambda \end{bmatrix} = \begin{bmatrix} 100 \\ 0.1 \end{bmatrix}, \begin{bmatrix} 10 \\ 0.1 \end{bmatrix}, \begin{bmatrix} 1 \\ 0.1 \end{bmatrix}, \begin{bmatrix} 1 \\ 1 \end{bmatrix}, \begin{bmatrix} 1 \\ 10 \end{bmatrix}.$$

The dependency of the parameter $\alpha = 0.4, 0.6, 0.8, 1.0, 1.2$ and 1.4 of the proposed method is shown in Fig. 4 for comparing with the LQR controller. The parameter β always takes the value of $1/100$ or less and we set $\beta = 0.01$ in this experiment. In principle, the parameter β is used in order to obtain a small initial velocity and to hold the particle at the final position.

In order to understand the difference of the two control strategies, we compared the strategies with respect to force transition. The force transitions of a reaching movement under the condition of the same settling time are shown in Fig. 6. The settling time is decided by the condition that a local standard deviation

$$\sigma(t) = \sqrt{\frac{\sum_t^{t+\Delta s} (x(t) - \bar{x}_f)^2}{\Delta s^2}} \text{ takes } < 0.01$$

and the time step Δs is 100. The settling time is $t_f = 2003$ in the case of the LQR controller $\eta = 1, \lambda = 1$, and $t_f = 1995$ in the case of the proposed method $\alpha = 0.8$. By comparing the torque cost function $J = (1/2) \int_0^{t_f} \vec{\tau}^T \vec{\tau}\, dt = (1/2) \int_0^{t_f} f_x^2\, dt$, which was used as a performance function of the multi-link movement strategy, the LQR controller shows $J_{PD} = 10.538$ and the proposed controller shows $J_{bell} = 5.975$. This means that an improvement of approximately 45% is found and this improvement has a tendency to disappear when the settling time becomes long. The strategic difference from the LQR control in the initial movement is

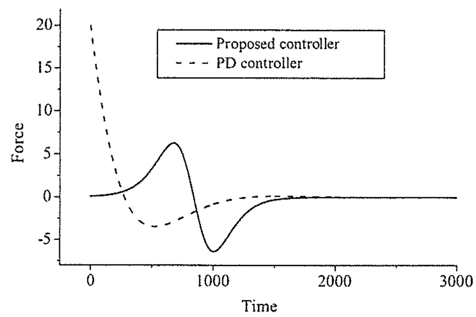

Figure 6. Comparison of the force transition between the proposed controller and the LQR controller.

emphasized in the case of a short settling time condition. This mechanism is useful for constructing a low-damage movement control system, and a reasonable and unstrained movement for a biological system.

The proposed controller, however, cannot manage with external disturbances such as gravity effects, and we introduce a compensator against external disturbances. If the motion equation of the particle is represented as $m\ddot{x}(t) + k\dot{x}(t) + d(t) = f(t)$, the force $f(t)$ is adjusted by:

$$\frac{\mathrm{d}f}{\mathrm{d}t} = -\gamma\left[m\ddot{x} + k\dot{x} - D(t)\right],$$
$$D(t) = \alpha\left\|\frac{\mathrm{d}x}{\mathrm{d}t}\right\| \cdot (x_r - x) + \beta \cdot (x_f - x), \tag{2}$$

where γ is a positive constant and $D(t)$ is the proposed control term. This works as a simple external disturbance compensator. Since this mechanism needs the present particle acceleration $\ddot{x}(t)$ and velocity $\dot{x}(t)$, we must know the information by observing sensors.

2.2. *Trajectory realization controller*

The motion equation of a two-link system (Fig. 7) is represented as:

$$M(\vec{q})\ddot{\vec{q}} + C\left(\dot{\vec{q}}, \vec{q}\right)\dot{\vec{q}} = \vec{\tau}, \tag{3}$$

where $\vec{q} = (\theta_1, \theta_2)$ represents the joint angle, $M \in R^{2\times2}$ is an inertia matrix, $C(\dot{\vec{q}}, \vec{q}) \in R^{2\times2}$ is a centrifugal, Coriolis and friction force, and $\vec{\tau} = (\tau_1, \tau_2)$ is a joint torque generated by agonist and antagonist muscles.

First, the process of the proposed controller is to derive a direct relation within the angular acceleration vector $\ddot{\vec{q}}$ and the torque $\vec{\tau}$, which is extracted from the motion equation (3):

$$\vec{\tau} = M(\vec{q})\ddot{\vec{q}}. \tag{4}$$

This simplification does not consider the effect of Coriolis, friction or centrifugal forces. If we can measure the precise joint friction or the centrifugal effect acting on a robot or a creature, then the inverse dynamics will be important for the torque decision process. The inverse dynamics problem is, however, difficult practically and does not work effectively in most real-world reaching movement process. Conversely, this simplification does not consider those dynamics positively, but rather is compensated for by the trajectory planning controller through the acceleration information of the end-effector.

Second, the end-effector position in 2D space (Fig. 7) is represented as:

$$\vec{x} = \begin{pmatrix} l_1\cos\theta_1 + l_2\cos(\theta_1+\theta_2) \\ l_1\sin\theta_1 + l_2\sin(\theta_1+\theta_2) \end{pmatrix}. \tag{5}$$

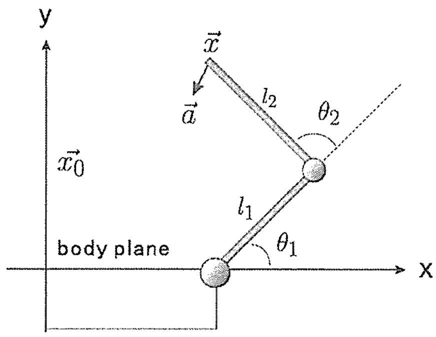

Figure 7. Two-link arm model in 2D space.

The acceleration of the end-effector can be calculated from (5) by taking the time derivative:

$$\vec{a} = \begin{pmatrix} a_x \\ a_y \end{pmatrix} = \begin{pmatrix} -l_1 \cos\theta_1 \dot{\theta}_1^{\,2} - l_1 \sin\theta_1 \ddot{\theta}_1 \\ -l_2 \cos(\theta_1 + \theta_2)(\dot{\theta}_1 + \dot{\theta}_2)^2 \\ -l_2 \sin(\theta_1 + \theta_2)(\ddot{\theta}_1 + \ddot{\theta}_2) \\ -l_1 \sin\theta_1 \dot{\theta}_1^{\,2} + l_1 \cos\theta_1 \ddot{\theta}_1 \\ -l_2 \sin(\theta_1 + \theta_2)(\dot{\theta}_1 + \dot{\theta}_2)^2 \\ +l_2 \cos(\theta_1 + \theta_2)(\ddot{\theta}_1 + \ddot{\theta}_2) \end{pmatrix}, \tag{6}$$

where l_1 and l_2 are the length from the shoulder to the elbow and from the elbow to the hand, respectively, and θ_1 and θ_2 are the angles of the shoulder and the elbow, respectively.

The third process is to define the cost function of the proposed method:

$$J = \|\vec{f} - \mu\vec{a}\|^2 = (f_x - \mu a_x)^2 + (f_y - \mu a_y)^2, \tag{7}$$

where $\vec{f}$ indicates the multi-dimensional form of the proposed trajectory planning algorithm (2), which is rewritten as:

$$\begin{aligned} \frac{\mathrm{d}\vec{f}}{\mathrm{d}t} &= -\gamma\left[m\ddot{\vec{x}} + k\dot{\vec{x}} - \vec{D}(t)\right], \\ \vec{D}(t) &= \alpha\left\|\frac{\mathrm{d}\vec{x}}{\mathrm{d}t}\right\| \cdot (\vec{x}_\mathrm{r} - \vec{x}) + \beta \cdot (\vec{x}_\mathrm{f} - \vec{x}), \end{aligned} \tag{8}$$

where $\vec{a}$ is the end-effector acceleration of (6) and μ is a positive constant.

In the control strategy, each joint torque is decided in order to minimize the cost function J and the least descent method is used for this purpose:

$$\begin{aligned} \vec{\tau}(t + \Delta t) &= \vec{\tau}(t) + \Delta\vec{\tau} \\ \Delta\vec{\tau} &= -\zeta\frac{\mathrm{d}J}{\mathrm{d}\vec{\tau}}, \end{aligned} \tag{9}$$

where ζ is a positive constant and Δt is a small time step. According to (9), the cost function value can be reduced in a step-by-step manner. The term $\mathrm{d}J/\mathrm{d}\vec{\tau}$ is calculated from:

$$\frac{\mathrm{d}J}{\mathrm{d}\vec{\tau}} = \frac{\mathrm{d}J}{\mathrm{d}\vec{a}} \cdot \frac{\mathrm{d}\vec{a}}{\mathrm{d}\vec{\tau}} = \frac{\mathrm{d}J}{\mathrm{d}\vec{a}} \cdot \frac{\mathrm{d}\vec{a}}{\mathrm{d}\ddot{\vec{\theta}}} \cdot \frac{\mathrm{d}\ddot{\vec{\theta}}}{\mathrm{d}\vec{\tau}}, \tag{10}$$

using (4), (6) and (7).

Previously proposed models, such as equilibrium control [14], control all joint angles so as to follow an ideal trajectory plan for all joint angles in angular space coordinate. In contrast, the proposed method uses only the ideal trajectory of the end-effector of the multi-link system in work space coordinates. Experimental results [8, 17] for a biological system using a 'work space coordinate', rather than an 'angular space coordinate', have shown a certain validity. These experiments demonstrate that a visual coordinate, i.e., the arm position from the viewing eye, is used for control in biological systems. The advantage of not using angular space coordinates is avoiding the accumulation error by increasing the number of links, avoiding the singularity of the inverse dynamics and eliminating the need to precisely decide the friction or the viscosity by observation of the system. In contrast, the advantage of using the work space coordinates is that considering the spatial position of the arm is easier than considering the angular space coordinates. Treating the end-effector position as the center of the control point avoids the need to manage the entire link system dynamics and simplifies the control problem, reducing the computational cost.

3. TWO-LINK ARM MOVEMENT

The reaching movement control experiment for a two-link system in 2D space, which is the simplest redundant system, is shown in Fig. 8. Here, $l_1 = 40, l_2 = 40, m_1 = 10, m_2 = 10$, the joint frictions are $k_1 = 600$ and $k_2 = 600$, and the time step is $\Delta t = 0.001$. The control parameters are $\alpha = 0.7$, $\beta = 0.01$, $\mu = 1.0$ and $\gamma = 10$. In addition, the bell-shaped speed profile control parameters are $\alpha = 1.0$ and $\beta = 0.01$, and the cost function parameter μ is 1.0. Figure 8a shows the results of the reaching movement control experiment for the case in which the initial position $\vec{x}_{\mathrm{i}} = (4.7, 13.1)$ is the position of the right hand in front of the body and the target position $\vec{x}_{\mathrm{f}} = (41.5, 68.3)$ is the position of the right hand stretched to the front-right of the initial position. The results of this experiment show that the trajectory path of the bell-shaped speed profile distribution of the end-effector is extended slightly upward.

Figure 8b shows the case in which the initial position is $\vec{x}_{\mathrm{i}} = (0, 14)$ and the target position is $\vec{x}_{\mathrm{f}} = (0.036, 46.48)$. This movement is such that the arm is stretched forward from the initial position. The movement shows an almost perfect bell-shaped speed profile pattern and the trajectory of the end-effector is almost a straight line. Figure 8c shows the case in which the arm is stretched to the front-right from the initial position. The trajectory shows a slight swell compared to the

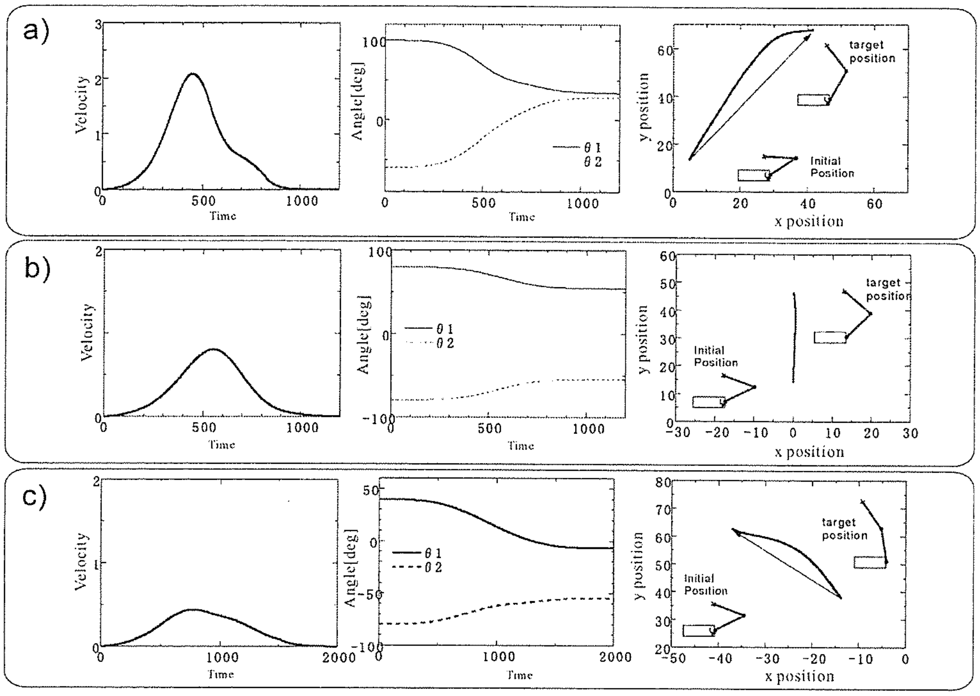

Figure 8. Two-link arm reaching movements in 2D space. Stretching direction: (a) front-right, (b) front and (c) front-left. The graphs give the speed profile of the end-effector, the angle transition and the position of the end-effector from the left.

movement to the front-right and the velocity profile is more similar to the bell-shape of the movement to the front. These trajectory shape features have been reported in Refs [8, 17, 21].

4. DEPENDENCY OF THE CONTROL SPEED

In the two-link reaching movement control under gravity the parameters are same as the two-link movement in a horizontal plane, except for $\alpha = 0.1$ (slow) and $\alpha = 0.3$ (fast) conditions, as shown in Fig. 9. Even under gravity, the proposed control strategy (7) and (9) requires no changes. However, the motion equation of the arm under gravity is of the form:

$$M(\vec{q})\ddot{\vec{q}} = C(\vec{q}, \dot{q}) + \vec{G} + \vec{\tau}, \tag{11}$$

where the term $\vec{G}$ is the gravity force element related to the shoulder and elbow angles θ_1 and θ_2, respectively. In this experiment, the initial position is equivalent to the arm being parallel to the line of the body and the target position is at approximately shoulder height, perpendicular to the line of the body. The trajectory of the end-effector is arc-shaped and is affected by gravity. In addition, the velocity profile of the arm is approximately bell-shaped, not perfectly bell-shaped.

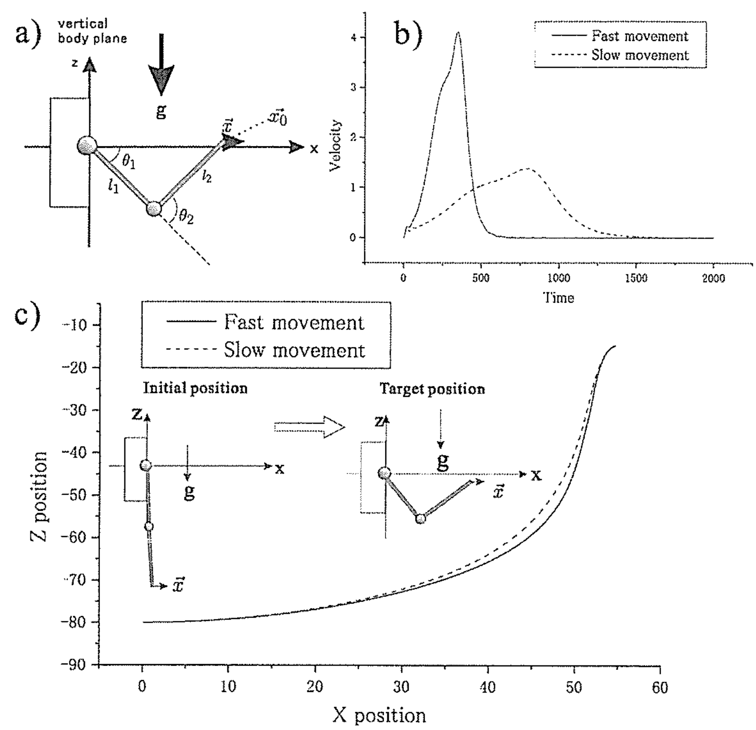

Figure 9. Two-link arm reaching movement under gravity in 2D space. (a) Diagram of the two-link model. (b) Velocity dependency of the different speed movement controls. (c) The realized trajectory patterns of the end-effector of the hand.

Concerning the dependency of the link movement speed, the trajectory transition of the end-effector (Fig. 9b) shifts slightly to the right (the front of the body) when the fast and the slow movement speeds are compared with respect to the inertia of the link movement.

5. STANDING-UP MOVEMENT OF A FOUR-LINK MODEL

In order to demonstrate the effectiveness of the proposed method for redundant manipulator control, we constructed a four-link model system (Fig. 10c) and confirmed the model using a standing-up movement from a chair. The averages of eight subjects reported in Ref. [22] were used for each of the link parameters (mass and moment) in the present experiment. The result of normal speed standing-up movement of a four-link model is shown in Fig. 10. In this simulation, the center of the gravity (COG) of the four-link model is considered as the end-effector of the arm and the movement is realized by moving the COG position. The parameters of the bell-shaped speed profile control are $\alpha = 1.0$ and $\beta = 0.01$, and the cost function parameter, J, is $\mu = 1.0$. The coordinates given for the model are the